Front. Earth Sci. 2014, 8(1): 115–122
DOI 10.1007/s11707-013-0364-0

RESEARCH ARTICLE

Transport of a volatile contaminant in a free-surface wetland flow

Jue YUAN[1], Li ZENG (✉)[1], Yijun ZHAO[1], Yihong WU[1], Ping JI[1], Bin CHEN[2]

1 State Key Laboratory of Simulation and Regulation of Water Cycle in River Basin, China Institute of Water Resources and Hydropower Research, Beijing 100038, China
2 State Key Laboratory of Water Environment Simulation, School of Environment, Beijing Normal University, Beijing 100875, China

Abstract Presented in this paper is an analytical study of a pulsed volatile contaminant emission into a free-surface wetland flow. A simplified model is given for contaminant transport under the combined action of advection, mass dispersion, apparent reaction, and volatilization at the free water surface. The effect of periodic apparent reaction on contaminant transport is separated from the hydraulic effect via an extended transformation, with a limiting case covering the known transformation for constant apparent reaction rate. The analytical solutions of zeroth and first order concentration moments are rigorously derived and illustrated. It was found that the amount of contaminant decreases from the bottom bed to the free-surface under volatilization, and the total amount of contaminant decays with time. It was also found that the moving speed of the mass center of the whole contaminant cloud increases, as the ratio of volatilization coefficient to vertical effective mass dispersivity increases.

Keywords contaminant transport, volatilization, reaction, wetland hydraulics

1 Introduction

The mechanism of contaminant transport in wetland flows has received increasing attention, due to its significant value for environmental risk assessment associated with wetlands (Mitsch and Gosselink, 1993; Costanza et al., 1997; Chen et al., 2009; Shao et al., 2012).

Contaminant transport in wetland flows is dependent on various factors, such as velocity distribution, apparent reaction, volatilization at the interface of water and air, infiltration at the bottom bed, etc. With respect to contaminant transport due to pure velocity distribution, some efforts have been made (Lightbody and Nepf, 2006a, b; Murphy et al., 2007; Nepf et al., 2007; Chen et al., 2010, 2012; Zeng, 2010; Wu et al., 2011a, b, 2012; Zeng et al., 2011, 2012a, b) based on Taylor's classic analysis of dispersion (Taylor, 1953), the method of concentration moments (Aris, 1956), and the multi-scale analysis method (Mei et al., 1996). In realistic wetland flows, there are various complex reactions, such as absorption, desorption, hydrolysis, etc., which are important to contaminant transport. Zeng and Chen (2011) analyzed the effect of apparent reaction rate on contaminant dispersion based on an ecological transformation, in which apparent reaction rate is assumed to be constant. However, the apparent reaction rate may change due to changes of temperature, salinity, etc. The effect of variations in apparent reaction rate over time on contaminant transport in wetland flows has not been well understood.

Municipal sewage and industrial wastewater may contain various volatile contaminants, such as dimethylsulfide, dimethyldisulfide, etc. When the contaminants are discharged into a wetland flow, they may escape from the water into the air by volatilization. Up to now, the effects of volatilization on the transport of contaminants in wetland flows has not been well understood.

This paper presents a theoretical analysis of the transport of volatile contaminants for a typical case involving a pulsed volatile contaminant emission into a free-surface wetland flow. The specific objectives are: (i) to obtain a transformation to separate the effect of periodic apparent reaction from the hydraulic effect, (ii) to present analytical solutions for the zeroth and first order concentration moments for volatile contaminants, and (iii) to illustrate the effect of characteristic parameters, associated with apparent reaction and volatilization, on contaminant transport.

Received January 4, 2013; accepted February 4, 2013

E-mail: lizeng0914@163.com

2 Formulation

The governing equation for the mass transport of a volatile contaminant in typical wetland flows is shown below (Liu and Masliyah, 2005; Zeng and Chen, 2011).

$$\phi\frac{\partial C}{\partial t}+\nabla\cdot(uC) =\nabla\cdot(\kappa\lambda\phi\nabla C)+\kappa\nabla\cdot(K\cdot\nabla C)-\phi k_a C, \quad (1)$$

where ϕ is porosity, t is time, C is contaminant concentration, u is velocity, κ is tortuosity, λ is mass diffusivity, K is mass dispersivity tensor, and k_a is apparent reaction rate. In realistic wetland flow situations, the apparent reaction rate may change with time. In this paper, we express a periodic apparent reaction rate with

$$k_a = k_s + k_o f(t), \quad (2)$$

where k_s is the steady component of the apparent reaction rate, k_o is the amplitude of the oscillatory component of the apparent reaction rate, and $f(t)$ is a periodic function with periodic average equal to zero.

Consider the transport of a volatile contaminant in a fully developed free-surface wetland flow in a Cartesian coordinate system, as shown in Fig. 1. The longitudinal x-axis is parallel to the flow direction, the vertical z-axis is upward, and the origin is located at the bottom bed. The solution for velocity distribution is (Zeng and Chen, 2011).

$$u(z) = U\frac{\cosh\alpha-\cosh[\alpha(1-z/H)]}{(\alpha\cosh\ \alpha-\sinh\ \alpha)/\alpha}, \quad (3)$$

where U is the depth-averaged velocity, and α is a dimensionless characteristic parameter.

Consider a uniform instantaneous discharge of a volatile contaminant at the position of $x=0$ at time $t=0$. The corresponding initial condition can be written as (Zeng and Chen, 2011)

$$C(x,z,t)|_{t=0} = \frac{Q}{\phi H}\delta(x), \quad (4)$$

where Q is the mass per unit width, and $\delta(x)$ is the Dirac delta function.

For the two-dimensional process, Eq. (1) reduces to

$$\frac{\partial C}{\partial t}+\frac{u}{\phi}\frac{\partial C}{\partial x} =\kappa\left[\lambda+\frac{K_L}{\phi}\right]\frac{\partial^2 C}{\partial x^2}+\kappa\left[\lambda+\frac{K_V}{\phi}\right]\frac{\partial^2 C}{\partial z^2} -k_s[1+\sigma f(t)]C, \quad (5)$$

where K_L and K_V are the longitudinal and vertical mass dispersivities, respectively; and $\sigma=k_o/k_s$ is the ratio of the steady component to the amplitude of the oscillatory component.

Since the discharge amount of the volatile contaminant is definite, the concentration boundary conditions at $x=\pm\infty$ are

$$C(\pm\infty,z,t) = 0, \quad (6)$$

assuming that the ambient concentration of the volatile contaminant in the air is equal to zero. For the impermeable bottom bed at $z=0$, and the free surface at $z=H$, the concentration boundary conditions are

$$\left.\frac{\partial C}{\partial z}\right|_{z=0} = 0,\ \left.\left[-\kappa\left(\lambda+\frac{K_V}{\phi}\right)\frac{\partial C}{\partial z}\right]\right|_{z=H} = (h_s C)|_{z=H}, \quad (7)$$

where h_s is the volatility coefficient, which is similar to a heat transfer coefficient.

The governing equation, as well as the boundary and initial conditions, can be rewritten in dimensionless form as

$$\frac{\partial\Omega}{\partial\tau}+\frac{Pe_x R_x^K}{\phi}\psi\frac{\partial\Omega}{\partial\xi} =R_x^K\frac{\partial^2\Omega}{\partial\xi^2}+\frac{\partial^2\Omega}{\partial\zeta^2}-N[1+\sigma\theta(\tau)]\Omega, \quad (8)$$

$$\Omega(\pm\infty,\zeta,\tau) = 0, \quad (9)$$

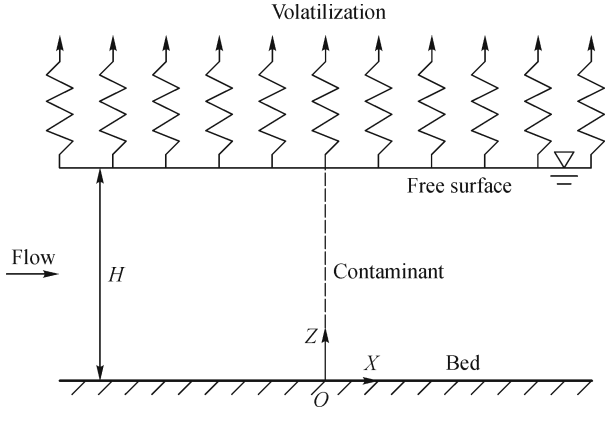

Fig. 1 Sketch for a free-surface wetland flow under volatilization.

$$\left.\frac{\partial\Omega}{\partial\zeta}\right|_{\zeta=0}=0,\qquad \left.\left[R_s\Omega+\frac{\partial\Omega}{\partial\zeta}\right]\right|_{\zeta=1}=0, \tag{10}$$

$$\Omega(\xi,\zeta,\tau)|_{\tau=0}=H\delta(H\xi), \tag{11}$$

where:

$$\begin{aligned}\xi=&\frac{x}{H},\ \zeta=\frac{z}{H},\ \tau=\frac{\kappa(\lambda+K_V/\phi)t}{H^2},\ \Omega(\xi,\zeta,\tau)=\frac{\phi CH^2}{Q},\\ Pe_x=&\frac{UH}{\kappa(\lambda+K_L/\phi)},\ R_x^K=\frac{\lambda+K_L/\phi}{\lambda+K_V/\phi},\\ \psi=&\frac{\alpha\{\cosh\alpha-\alpha\cosh[\alpha(\zeta-1)]\}}{\alpha\cosh\ \alpha-\sinh\ \alpha},\\ \theta(\tau)=&f\left(\frac{H^2\tau}{\kappa(\lambda+K_V/\phi)}\right),\ \ R_s=\frac{Hh_s}{\kappa(\lambda+K_V/\phi)}.\end{aligned} \tag{12}$$

The dimensionless parameter R_s reflects the relative strength of volatilization, and the effective mass dispersion in the vertical direction.

3 Separation of the effect of periodic apparent reaction from the hydraulic effect

The dimensionless concentration determined by Eqs. (8)–(11) is dependent on advection, mass dispersion, apparent reaction, and volatilization. For the case of constant apparent reaction rate, the effect of apparent reaction can be separated from the hydraulic effect by a simple exponential transformation (Zeng and Chen, 2011). For the case of periodic apparent reaction rate, an extended exponential transformation equation,

$$\Omega(\xi,\zeta,\tau)=\Omega^*(\xi,\zeta,\tau)\exp\left(\int_0^\tau -N[1+\sigma\theta(\tau_1)]\mathrm{d}\tau_1\right), \tag{13}$$

was used to separate the effect of apparent reaction from the hydraulic effect, where $\Omega^*(\xi, \zeta, \tau)$ is only dependent on advection, mass dispersion, and volatilization. The transformation given by Zeng and Chen (2011) can be included as a special case of $\sigma=0$. With Eq. (13), we have

$$\frac{\partial\Omega^*}{\partial\tau}+\frac{Pe_xR_x^K}{\phi}\psi\frac{\partial\Omega^*}{\partial\xi}=R_x^K\frac{\partial^2\Omega^*}{\partial\xi^2}+\frac{\partial^2\Omega^*}{\partial\zeta^2}, \tag{14}$$

$$\Omega^*(\pm\infty,\zeta,\tau)=0, \tag{15}$$

$$\left.\frac{\partial\Omega^*}{\partial\zeta}\right|_{\zeta=0}=0,\ \left.\left(R_s\Omega^*+\frac{\partial\Omega^*}{\partial\zeta}\right)\right|_{\zeta=1}=0, \tag{16}$$

$$\Omega^*(\xi,\zeta,\tau)|_{\tau=0}=H\delta(H\xi). \tag{17}$$

To illustrate the effect of time-dependent apparent reaction rate on contaminant transport, three kinds of apparent reaction rate were considered. The first case is where $\theta(\tau)=|\cos(\tau)|$, which means that ambient factors strengthen the apparent reaction all the time. The second case is where $\theta(\tau)=-|\cos(\tau)|$, which means that the ambient factors weaken the apparent reaction all the time. The third case is where $\theta(\tau)=\cos(\tau)$, which means that the ambient factors strengthen and weaken the apparent reaction periodically.

Figure 2 shows the variation of Λ_1 with τ for $N=1$, and $\sigma=0.1$, 0.2, and 0.3, where Λ_1 is expressed as

$$\Lambda_1=\frac{\Omega_1}{\Omega_0}=\frac{\exp\left(\int_0^\tau -N[1+\sigma|\cos(\tau_1)|]\mathrm{d}\tau_1\right)}{\exp\left(\int_0^\tau -N\mathrm{d}\tau_1\right)}. \tag{18}$$

Ω_0 is the contaminant concentration corresponding to $\theta(\tau)=0$, and Ω_1 is the contaminant concentration corresponding to $\theta(\tau)=|\cos(\tau)|$. It is shown that Λ_1 decreases with time. For a given N, Λ_1 decreases with the increase of σ.

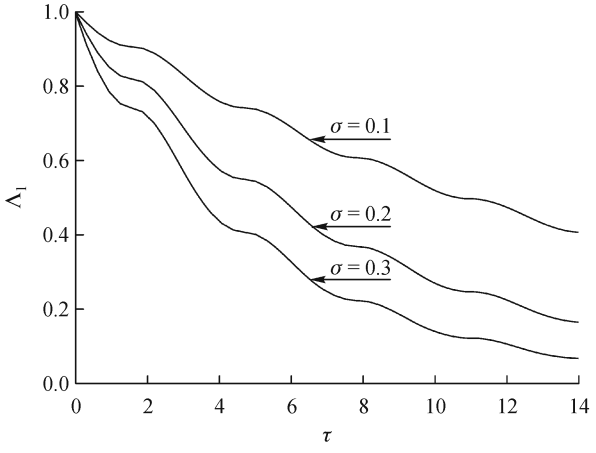

Fig. 2 Variation of Λ_1 with τ for $N=1$, and $\sigma=0.1$, 0.2, and 0.3.

Figure 3 shows the variation of Λ_2 with τ for $N=1$, and $\sigma=0.1$, 0.2, and 0.3, where Λ_2 is expressed as

$$\Lambda_2=\frac{\Omega_2}{\Omega_0}=\frac{\exp\left(\int_0^\tau -N[1-\sigma|\cos(\tau_1)|]\mathrm{d}\tau_1\right)}{\exp\left(\int_0^\tau -N\mathrm{d}\tau_1\right)}, \tag{19}$$

and Ω_2 is the contaminant concentration corresponding to $\theta(\tau)=-|\cos(\tau)|$. It is shown that Λ_2 increases with time. For a given N, Λ_2 increases with increases of σ.

Figure 4 shows the variation of Λ_3 with τ for $\sigma=0.1$, 0.2, 0.3, and $N=1$, where Λ_3 is expressed as

$$\Lambda_3=\frac{\Omega_3}{\Omega_0}=\frac{\exp\left(\int_0^\tau -N[1+\sigma\cos(\tau_1)]\mathrm{d}\tau_1\right)}{\exp\left(\int_0^\tau -N\mathrm{d}\tau_1\right)}, \tag{20}$$

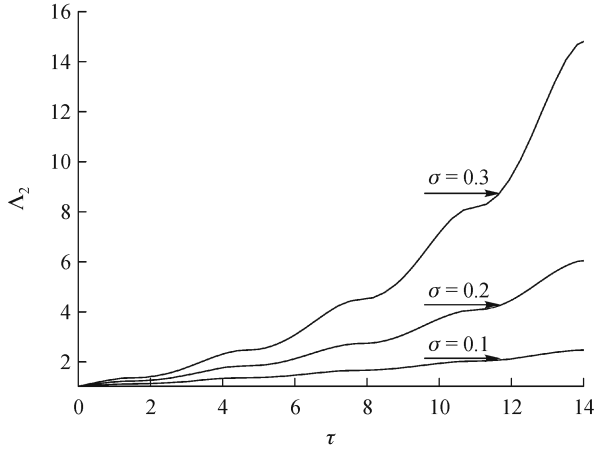

Fig. 3 Variation of Λ_2 with τ for $N = 1$, and $\sigma = 0.1$, 0.2, and 0.3.

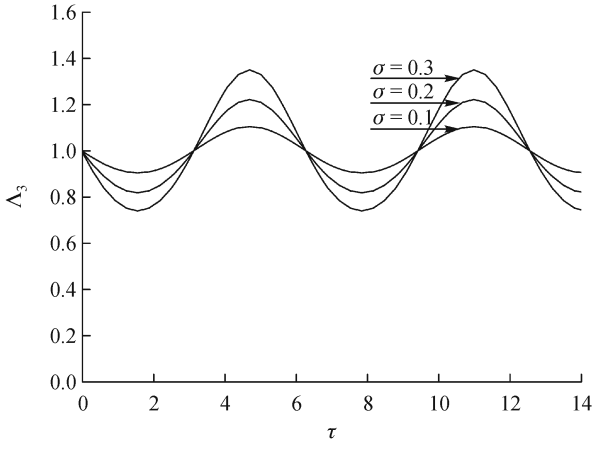

Fig. 4 Variation of Λ_3 with τ for $N = 1$, and $\sigma = 0.1$, 0.2, and 0.3.

and Ω_3 is the contaminant concentration corresponding to $\theta(\tau) = \cos(\tau)$. It is shown that Λ_3 changes periodically with time. For a given N, the amplitude of Λ_3 increases with increases of σ.

Figure 5 shows the variation of Λ_3 with τ for $\sigma = 0.2$, and $N = 0.5$, 1, and 2. It is shown that as N increases, the amplitude of Λ_3 increases.

4 Concentration moment analysis

The method of concentration moments (Aris, 1956) was adopted to analyze the transport of a volatile contaminant in a free-surface wetland flow. The zeroth order concentration moment m_0 and the first order concentration moment m_1 are defined respectively as

$$m_0 \equiv \int_{-\infty}^{\infty} \Omega^*(\xi,\zeta,\tau)\mathrm{d}\xi, \tag{21}$$

and

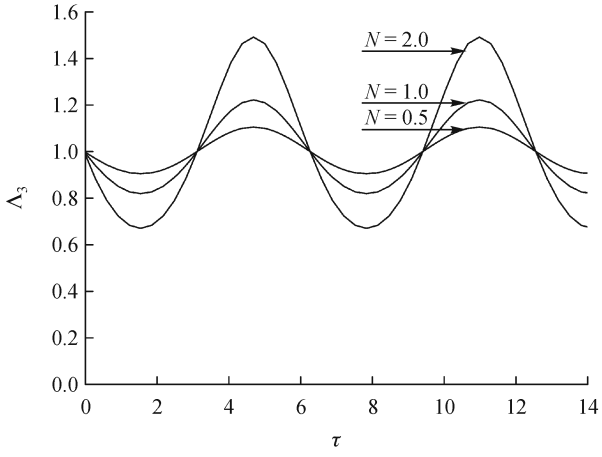

Fig. 5 Variation of Λ_3 with τ for $\sigma = 0.2$, and $N = 0.5$, 1, and 2.

$$m_1 \equiv \int_{-\infty}^{\infty} \Omega^*(\xi,\zeta,\tau)\xi\mathrm{d}\xi. \tag{22}$$

The zeroth and first order concentration moments reflect the amount of volatile contaminant, and the movement of the mass center of the contaminant cloud, respectively.

The concentration moments satisfy (Fried, 1975; Barton, 1983)

$$\xi\Omega^*|_{\xi=\pm\infty} = \frac{\partial\Omega^*}{\partial\xi}\bigg|_{\xi=\pm\infty} = \xi\frac{\partial\Omega^*}{\partial\xi}\bigg|_{\xi=\pm\infty} = 0. \tag{23}$$

Applying the operator $\int_{-\infty}^{\infty}(\cdot)\,\mathrm{d}\xi$ to Eqs. (8), (10), and (11), with the aid of Eqs. (9) and (23), we have

$$\frac{\partial m_0}{\partial\tau} = \frac{\partial^2 m_0}{\partial\zeta^2}, \tag{24}$$

$$\frac{\partial m_0}{\partial\zeta}\bigg|_{\zeta=0} = 0,\ \left(R_s m_0 + \frac{\partial m_0}{\partial\zeta}\right)\bigg|_{\zeta=1} = 0, \tag{25}$$

$$m_0(\zeta,\tau)|_{\tau=0} = 1. \tag{26}$$

Solving Eqs. (24)–(26), we have

$$m_0(\zeta,\tau) = \sum_{i=1}^{\infty} \frac{2(\beta_i^2 + R_s^2)\ \sin\beta_i}{\beta_i^2 + R_s^2 + R_s\quad\beta_i}\cos(\beta_i\zeta)\exp(-\beta_i^2\tau), \tag{27}$$

where β_i is determined by

$$\beta_i\tan\beta_i = R_s. \tag{28}$$

Table 1 presents the eigenvalues β_i ($i = 1$, 2, 3, 4, and 5) for $R_s = 0.25$, 0.5, 1.0, 2.0, and 4.0.

Figure 6 shows the variation of m_0 with ξ for $\tau = 0.1$, and $R_s = 0.25$, 0.5, 1.0, 2.0, and 4.0. Figure 7 shows the variation of m_0 with ξ for $\tau = 1$, and $R_s = 0.25$, 0.5, 1.0, 2.0, and 4.0. It is shown that m_0 decreases as ξ increases, which

Table 1 Eigenvalues β_i (i = 1, 2, 3, 4 and 5) for R_s = 0.25, 0.5, 1.0, 2.0, and 4.0

R_s	β_1	β_2	β_3	β_4	β_5
0.25	0.480094	3.219099	6.322705	9.451223	12.586231
0.5	0.653271	3.292311	6.361621	9.477486	12.606013
1.0	0.860334	3.425618	6.437299	9.529334	12.645287
2.0	1.076874	3.643597	6.578334	9.629560	12.722299
4.0	1.264592	3.935162	6.814010	9.811878	12.867756

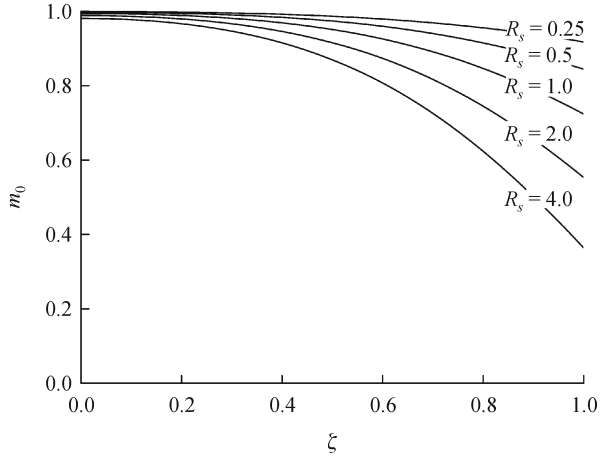

Fig. 6 Variation of m_0 with ξ for τ= 0.1, and R_s = 0.25, 0.5, 1.0, 2.0 and 4.0.

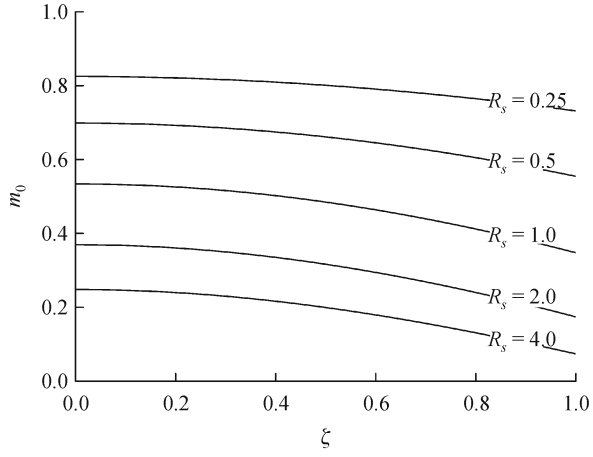

Fig. 7 Variation of m_0 with ξ for τ= 1, and R_s = 0.25, 0.5, 1.0, 2.0 and 4.0.

means that the amount of contaminant near the free-water surface is less than that near the bottom bed. The distribution of m_0 for the volatile contaminant is different from that for the non-volatile contaminant in the vertical direction, which stays constant (Zeng and Chen, 2011). At the initial stage, the volatilization has less effect on m_0 near the bottom bed. The effect of volatilization on m_0 gradually increases with time, and finally has an important impact on the whole cross-section.

The depth average of m_0 is

$$\overline{m}_0 = \sum_{i=1}^{\infty} \frac{2(\beta_i^2 + R_s^2)}{\beta_i^2 + R_s^2 + R_s} \left(\frac{\sin \beta_i}{\beta_i} \right)^2 \exp(-\beta_i^2 \tau). \tag{29}$$

Figure 8 shows the variation of $\overline{m}_0$ with τ for R_s = 0.25, 0.5, 0.75, 1.0, and 2.0. It is shown that $\overline{m}_0$ gradually decreases to zero. The dimensionless time scale for m_0 to decay fully is given by

$$\tau_c >> \frac{1}{\beta_1^2}, \tag{30}$$

and the corresponding dimensioned time scale is given by

$$t_c >> \frac{H^2}{\beta_1^2 \kappa(\lambda + K_V/\phi)}. \tag{31}$$

As R_s increases, $\overline{m}_0$ decreases. This result means that the total amount of volatile contaminant in the water body decreases, as volatilization increases.

Applying the operator $\int_{-\infty}^{\infty}(\cdot)\ \xi \mathrm{d}\xi$ to Eqs. (8), (10), and (11), with the aid of Eqs. (9) and (23), we have

$$\frac{\partial m_1}{\partial \tau} = \frac{\partial^2 m_1}{\partial \zeta^2} + \frac{Pe_x R_x^K \psi}{\phi} m_0, \tag{32}$$

$$\left.\frac{\partial m_1}{\partial \zeta}\right|_{\zeta=0} = 0, \left.\left(R_s m_1 + \frac{\partial m_1}{\partial \zeta}\right)\right|_{\zeta=1} = 0, \tag{33}$$

$$m_1(\zeta,\tau)|_{\tau=0} = 0. \tag{34}$$

Solving Eqs. (32)–(34), we have

$$m_1(\zeta,\tau) = \sum_{j=1}^{\infty}\sum_{i=1}^{\infty} \frac{Pe_x R_x^K}{\phi} \frac{2(\beta_j^2 + R_s^2)}{\beta_j^2 + R_s^2 + R_s} \frac{2(\beta_i^2 + R_s^2)}{\beta_i^2 + R_s^2 + R_s} \frac{\sin \beta_i}{\beta_i} \cdot (P_1 + P_2) P_3 \cos(\beta_j \zeta), \tag{35}$$

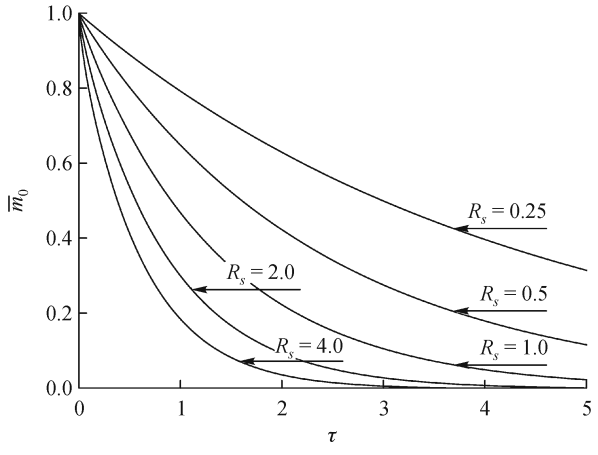

Fig. 8 Variation of $\overline{m}_0$ with τ for R_s = 0.25, 0.5, 0.75, 1.0, and 2.0.

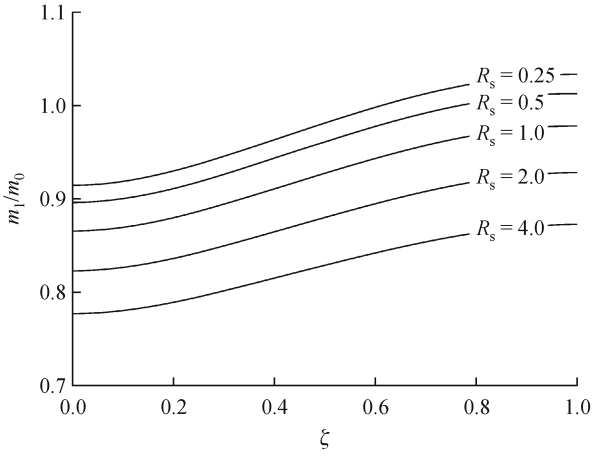

Fig. 9 Variation of m_1/m_0 with ξ for $Pe_xR_x^K/\phi = 1.0$, $\alpha = 1.0$, τ= 1.0 and R_s = 0.25, 0.5, 1.0, 2.0 and 4.0.

where P_1, P_2 and P_3 can be expressed respectively as

$$P_1 = \begin{cases} \dfrac{(\beta_i+\beta_j)\sin(\beta_i-\beta_j)+(\beta_i-\beta_j)\sin(\beta_i+\beta_j)}{2(\beta_i^2-\beta_j^2)(\cosh\alpha-\sinh\alpha/\alpha)/\cosh\alpha} & (i\neq j) \\ \dfrac{\sin(2\beta_i)+2\beta_i}{4\beta_i(\cosh\alpha-\sinh\alpha/\alpha)/\cosh\alpha} & (i=j) \end{cases}, \tag{36}$$

$$\begin{aligned} P_2 = &-\frac{(\beta_i+\beta_j)[(\beta_i-\beta_j)^2+\alpha^2]\sin(\beta_i+\beta_j)}{[2\alpha^4+2(\beta_i^2-\beta_j^2)^2+4\alpha^2(\beta_i^2+\beta_j^2)](\cosh\alpha-\sinh\alpha/\alpha)} \\ &-\frac{(\beta_i-\beta_j)[(\beta_i+\beta_j)^2+\alpha^2]\sin(\beta_i-\beta_j)}{[2\alpha^4+2(\beta_i^2-\beta_j^2)^2+4\alpha^2(\beta_i^2+\beta_j^2)](\cosh\alpha-\sinh\alpha/\alpha)} \\ &-\frac{2\alpha(\beta_i^2+\beta_j^2)\sinh\alpha+2\alpha^3\sinh\alpha}{[2\alpha^4+2(\beta_i^2-\beta_j^2)^2+4\alpha^2(\beta_i^2+\beta_j^2)](\cosh\alpha-\sinh\alpha/\alpha)}, \end{aligned} \tag{37}$$

and

$$P_3 = \begin{cases} \dfrac{-\exp(-\beta_j^2\tau)+\exp(-\beta_j^2\tau)}{\beta_j^2-\beta_i^2} & (i\neq j) \\ \tau\exp(-\beta_j^2\tau) & (i=j) \end{cases}. \tag{38}$$

Then we have

$$\overline{m}_1(\tau) = \sum_{j=1}^{\infty}\sum_{i=1}^{\infty}\frac{Pe_xR_x^K}{\phi}\frac{2(\beta_j^2+R_s^2)}{\beta_j^2+R_s^2+R_s}\frac{2(\beta_i^2+R_s^2)}{\beta_i^2+R_s^2+R_s} \frac{\sin\beta_i}{\beta_i}\frac{\sin\beta_j}{\beta_j}\cdot(P_1+P_2)P_3. \tag{39}$$

Figure 9 shows the variation of m_1/m_0 with ξ for $Pe_xR_x^K/\phi = 1.0$, $\alpha = 1.0$, τ= 1.0, and R_s = 0.25, 0.5, 1.0, 2.0, and 4.0. It is shown that $m_1/\overline{m}_0$ increases with ξ, which means that the mass center of a contaminant moves quickly on the streamline through ξ= 1.0.

Figure 10 shows the variation of $\overline{m}_1/\overline{m}_0$ with τ for $Pe_xR_x^K/\phi = 1.0$, $\alpha = 1.0$, and R_s = 0.25, 0.5, 1.0, 2.0, and 4.0. The mass center of the whole contaminant cloud will move longitudinally. The slope of the curves in Fig. 10 reflects the moving speed of the mass center. As volatilization increases, the moving speed decreases.

5 Conclusions

For free-water surface wetland flows, a simplified model has been given to reflect the effects of advection, mass dispersion, apparent reaction, and volatilization on contaminant transport.

The effect of periodic apparent reaction on contaminant transport is separated from the hydraulic effect via an extended transformation. The transformation for constant

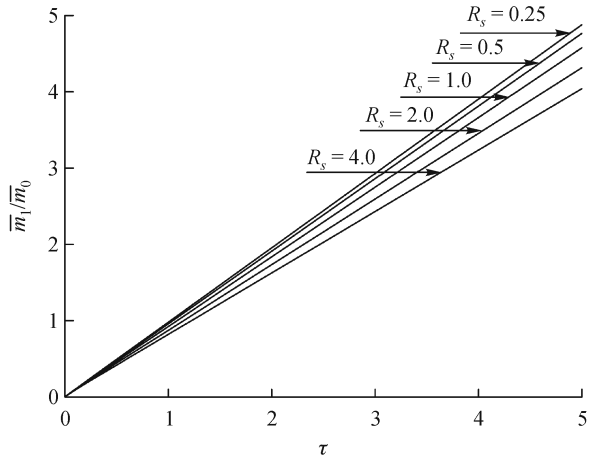

Fig. 10 Variation of $\overline{m}_1/\overline{m}_0$ with τ for $Pe_x R_x^K/\phi = 1.0$, $\alpha = 1.0$, and R_s = 0.25, 0.5, 1.0, 2.0 and 4.0.

apparent reaction rate can be included as a special case of $\sigma = 0$. For three cases, $\theta(\tau) = |\cos(\tau)|$, $-|\cos(\tau)|$, and $\cos(\tau)$, the effects of periodic reaction on contaminant transport are illustrated. It is shown that the oscillatory component of periodic apparent reaction rate may increase or decrease the contaminant concentration.

The method of concentration moments was used to obtain the zeroth and first order concentration moments. The distribution of m_0 for the volatile contaminant was different from that for the non-volatile contaminant in the vertical direction. The former kept constant, while the latter decreased from the bottom bed to the free water surface. The total amount of contaminant cloud decays with time. At the initial stage, the influenced range of volatilization for m_0 is limited to the bottom bed. For the long term evolution of a volatile contaminant, the influenced range spreads to the whole cross-section. It was found that the moving speed of the mass center of the contaminant on the streamline increases from the bottom bed to the free water surface. The moving speed of the mass center for the whole contaminant cloud decreases with increases of the ratio of volatilization coefficient to vertical effective mass dispersivity.

Acknowledgements This work is supported by the Special Foundation of China Institute of Water Resources and Hydropower Research (Contract No. Shuji1345).

References

Aris R (1956). On the dispersion of a solute in a fluid flowing through a tube. P Roy Soc Lond A Mat, 235(1200), 67–77

Barton N G (1983). On the method of moments for solute dispersion. J Fluid Mech, 126(1): 205–218

Chen G Q, Wu Z, Zeng L (2012). Environmental dispersion in a two-layer wetland: analytical solution by method of concentration moments. Int J Eng Sci, 51: 272–291

Chen G Q, Zeng L, Wu Z (2010). An ecological risk assessment model for a pulsed contaminant emission into a wetland channel flow. Ecol Model, 221(24): 2927–2937

Chen Z M, Chen G Q, Chen B, Zhou J B, Yang Z F, Zhou Y (2009). Net ecosystem services value of wetland: environmental economic account. Commun Nonlinear Sci Numer Simul, 14(6): 2837–2843

Costanza R, d'Arge R, de Groot R, Farber S, Grasso M, Hannon B, Limburg K, Naeem S, O'Neill R V, Paruelo J, Raskin R G, Sutton P, van den Belt M (1997). The value of the world's ecosystem services and natural capital. Nature, 387(6630): 253–260

Fried J J (1975). Groundwater Pollution: Theory, Methodology, Modelling and Practical Rules. Amsterdam: Elsevier Scientific Publishing Company

Lightbody A F, Nepf H M (2006a). Prediction of velocity profiles and longitudinal dispersion in emergent salt marsh vegetation. Limnol Oceanogr, 51(1): 218–228

Lightbody A F, Nepf H M (2006b). Prediction of near-field shear dispersion in an emergent canopy with heterogeneous morphology. Environ Fluid Mech, 6(5): 477–488

Liu S, Masliyah J H (2005). Dispersion in porous media. In: Vafai K ed. Handbook of Porous Media. Boca Ratton: CRC Press, 81–140

Mei C C, Auriault J L, Ng C O (1996). Some applications of the homogenization theory. In: Hutchinson J W, Wu T Y eds. Advances in Applied Mechanics. California: Academic Press, 277–348

Mitsch W J, Gosselink J G (1993). Wetlands (2nd ed). New York: Van Nostrand Reinhold

Murphy E, Ghisalberti M, Nepf H (2007). Model and laboratory study of dispersion in flows with submerged vegetation. Water Resour Res, 43 (5): W05438

Nepf H, Ghisalberti M, White B, Murphy E (2007). Retention time and dispersion associated with submerged aquatic canopies. Water Resour Res, 43(4): W04422

Shao L, Wu Z, Zeng L, Chen Z M, Zhou Y, Chen G Q (2012). Embodied energy assessment for ecological wastewater treatment by a constructed wetland. Ecol Model,doi: 10.1016/j.ecolmodel.2012.09.004

Taylor G (1953). Dispersion of soluble matter in solvent flowing slowly through a tube. P Roy Soc Lond A Mat, 219(1137): 186–203

Wu Z, Chen G Q, Zeng L (2011a). Environmental dispersion in a two-zone wetland. Ecol Modell, 222(3): 456–474

Wu Z, Li Z, Chen G Q (2011b). Multi-scale analysis for environmental dispersion in wetland flow. Commun Nonlinear Sci Numer Simul, 16 (8): 3168–3178

Wu Z, Zeng L, Chen G Q, Li Z, Shao L, Wang P, Jiang Z (2012). Environmental dispersion in a tidal flow through a depth-dominated wetland. Commun Nonlinear Sci Numer Simul, 17(12): 5007–5025

Zeng L 2010. Analytical Study on Environmental Dispersion in Wetland Flow. Disseration for Ph D degree. Beijing: Peking University (in Chinese)

Zeng L, Chen G, Wu Z, Li Z, Wu Y H, Ji P (2012a). Flow distribution and environmental dispersivity in a tidal wetland channel of rectangular cross-section. Commun Nonlinear Sci Numer Simul, 17

(11): 4192–4209

Zeng L, Chen G Q (2011). Ecological degradation and hydraulic dispersion of contaminant in wetland. Ecol Modell, 222(2): 293–300

Zeng L, Chen G Q, Tang H S, Wu Z (2011). Environmental dispersion in wetland flow. Commun Nonlinear Sci Numer Simul, 16(1): 206–215

Zeng L, Wu Y, Ji P, Chen B, Zhao Y J, Chen G Q, Wu Z (2012b). Effect of wind on contaminant dispersion in a wetland flow dominated by free-surface effect. Ecol Modell, 237–238: 101–108